Neurosurg. Rev.
11 (1988) 67–76

On the ultrastructure of ependymomas – A semiquantitative analysis of diagnostic criteria in 21 cases with special reference to glycogen as a marker

Jens Haustein, Felix Cruz-Sanchez, and Jose Cervós-Navarro

Institute for Neuropathology, Free University of Berlin, Berlin, West Germany

Abstract

We report our results on the ultrastructure of 21 ependymomas and establish the following diagnostic criteria: 1. Glycogen is the most frequently encountered criterion, followed by desmosomes, cilia, basal bodies and microvilli. Fifteen tumors had 3 or more of these features. 2. The allegedly typical nuclear pattern was found in only 6 cases. 3. Special ultrastructural features seen include basement membranes in a mid-thoracic ependymoma. Furthermore we propose the hypothesis that glycogen might be involved in cilia assembly.

Keywords: Electron microscopy, ependymoma, glycogen, ultrastructure.

1 Introduction

Ependymomas were first classified and differentiated by BAILEY [1], based on six of his own cases. He particularly emphasized that previous diagnoses had included a variety of other brain tumors. SVIEN et al. [30], from the group of Kernohan then suggested that a subclassification be made according to the degree of malignancy. The morphologic criteria were the occurrence of pleomorphism, hyperchromatism and pathological mitoses.

LUSE [22] published early electron microscope studies in 1960, and several authors subsequently confirmed the ultrastructural criteria in single cases [6, 7, 9, 12, 14, 24]. Characteristic were microvilli, cilia, elongated desmosomes and a typical nuclear structure. Observations on embryonal material, experimentally induced tumors and xenograft tumors were included in the evalution of the ultrastructural findings [13, 16, 25].

Nevertheless, there remain questions which cannot be answered by histological methods, even after the inclusion of newer techniques. One drawback is the fact that almost all reports consider single or small groups of cases. Recently we presented data on the histopathology of ependymoblastomas [3, 4]; related histological work has been done including the cases presented here (5). It is the aim of the present report to investigate to what extent electron microscopy can aid the diagnosis of ependymomas.

2 Materials and methods

In all cases the tumor material was obtained by biopsy. The clinical data are summarized together with the histological diagnosis in Table I. Material from 21 tumors was prepared for electron microscopy. Tissue samples were fixed in 3.5% buffered glutaraldehyde solution for 4 hours, washed in 0.2 M sucrose and post-fixed in 1% osmium tetroxide solution for 1 hour. After dehydration in the alcohol series, the samples were embedded in Mikropal or araldite. Semithin sections cut from 4–8 blocks were examined. After elimination of hematoma or necrotic areas, ultrathin sections were prepared with a Reichert microtome and stained with lead citrate or uranyl acetate.

3 Results

Histological landmarks are perivascular halos und rosettes (Figure 1). The tumor cells usually occur in small mosaic-like groups, occasionally separate from each other (Figure 2). A variable number of cell processes push their way between neighboring perikarya – in some areas these processes constitute the mayor part of the tumor. They often spread to the vascular basal membrane and thereby run parallel to each other. Undifferentiated cells comprise a large part of the cell population (Figure 3). The perikaryon consists of a narrow band of cytoplasm, rarely wider than 2 μm. It may contain christae-type mitochondria, lysosomes, little rER, free ribosomes and polysomes. Occasionally the Golgi complex is well developed. Rosette formation (Figures 2, 4, and 5) occurred in the following combinations: rosettes

Table I. Clinical data and histological results

Case	Age/Sex	History	Localization	LM diagnosis
1	26/F	4 mo	L temporal intraventricular	E I
2	48/M	4 mo	R parasellar	E I
3	44/F	1 mo	3rd ventricle	E I
4	7/M	–	L temporobasal to brainstem	E I
5	62/F	3 wk	L occipital paramedian	E I
6	16/F	–	–	E I
7	46/M	2 yr	Th 3–8	E I
8	65/M	3 mo	Th 7–8	E I, relapse after 2 years
9	10/M	–	L 4 extradural	E I
10	24/–	–	S 1	E I
11	27/–	–	L parietal	E I
12	28/M	3 wk	R frontotemporal connected to ventricle	E III–IV, relapse after 2 years
13	40/F	6 mo	R frontotemporal	E III–IV, relapse after 14 years
14	45/M	3 wk	R precentral	E III–IV
15	59/M	1 wk	L temporo-occipital connected to ventricle	E III–IV
16	8 mo/F	2 mo	L cerebellar hemisphere	E III–IV
17	8/M	2 mo	cranio-cervical cord to floor of 4th ventricle	E III–VI
18	49/M	5 yr	R cerebellar hemisphere tentorium incisure	E III–IV
19	44/F	–	–	E III–IV
20	4/F	–	–	E III–IV
21	14/F	1 yr	pineal region	E III–IV

Negative (–): no data; L-left; R-right; E-ependymoma

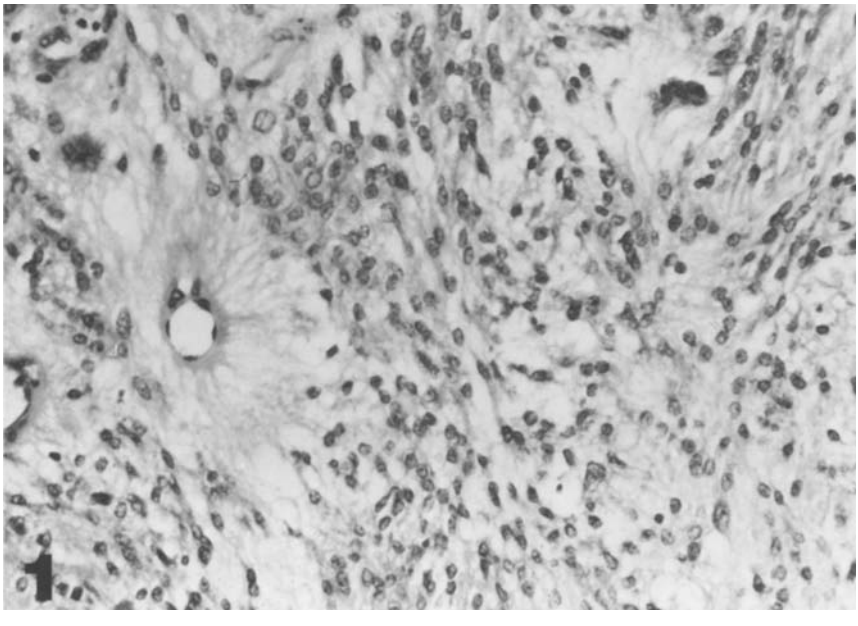

Figure 1. Light micrograph of a typical area of one of the spinal tumors showing perivascular halo. Case 7. HE x 150.

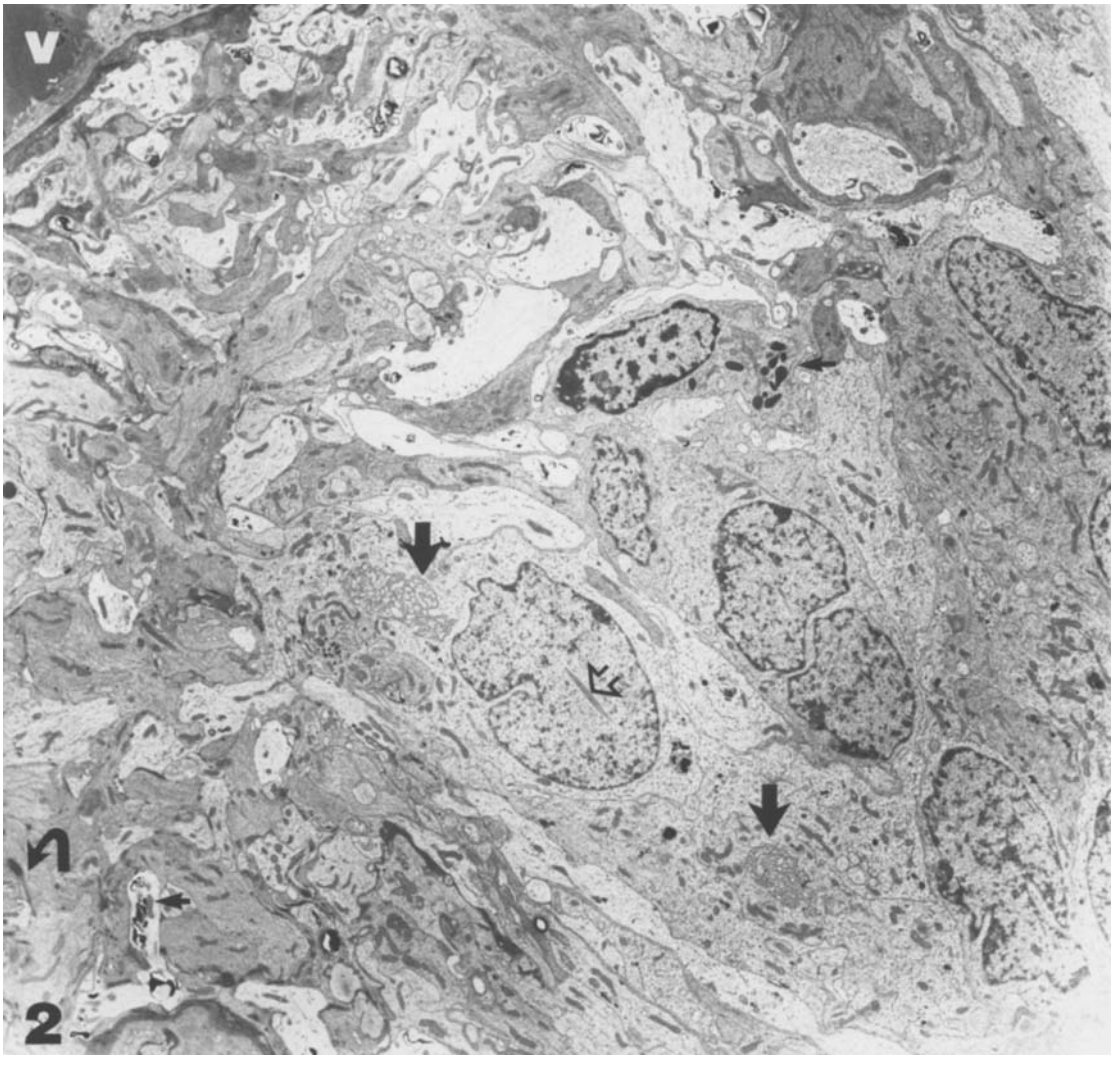

Figure 2. General tumor morphology: cell-free perivascular zone, vessel (v), ultrastructural rosettes (arrows), cilium (curved arrow), nuclear inclusions (open arrow), dense bodies (small arrows). Case 19, x 1.700.

with microvilli, elongated desmosomes and cilia (5 cases); with microvilli and elongated desmosomes (3 cases); with microvilli (2 cases); with elongated desmosomes (1 case). In the first three combinations, the central lumen is usually completely filled with microvilli, an empty lumen is rare. Basal bodies are often also present. Some nuclei contain intranuclear bundles of 8 nm filaments which have neither a halo nor contact with the nucleolus or nuclear membrane (Figure 2). Considerable irregularities are seen in malignant variants, including lapped nuclei and chromatin clumping. We found mitoses in 6 of the grade III–IV tumors.

Intracytoplasmic 10 nm wide filaments are distributed evenly throughout the perikaryon but are particularly numerous in the cell processes. One of the spinal tumors showed a particularly dense accumulation of filamentous material in the perikaryon, surrounding the entire nucleus and displacing the other cytoplasmic organelles to the periphery.

In 14 cases we found glycogen (Figures 4–10), partly in alpha- oder beta granule form, distributed throughout the cytoplasm and in the cell processes. As well as this more diffuse distribution, glycogen was also found in more concentrated pools which

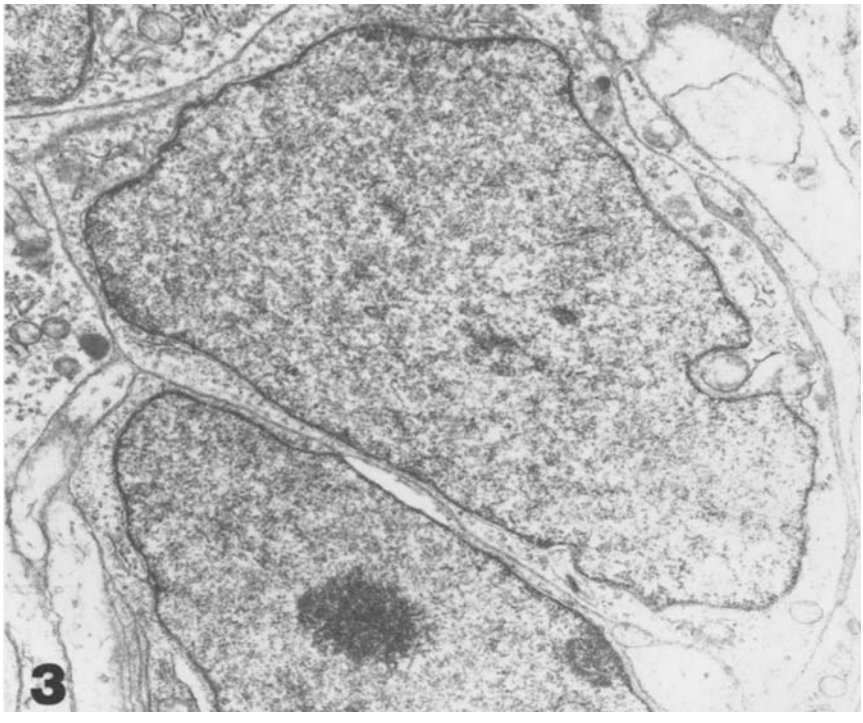

Figure 3. Undifferentiated tumor cells. Case 4, x 2.600.

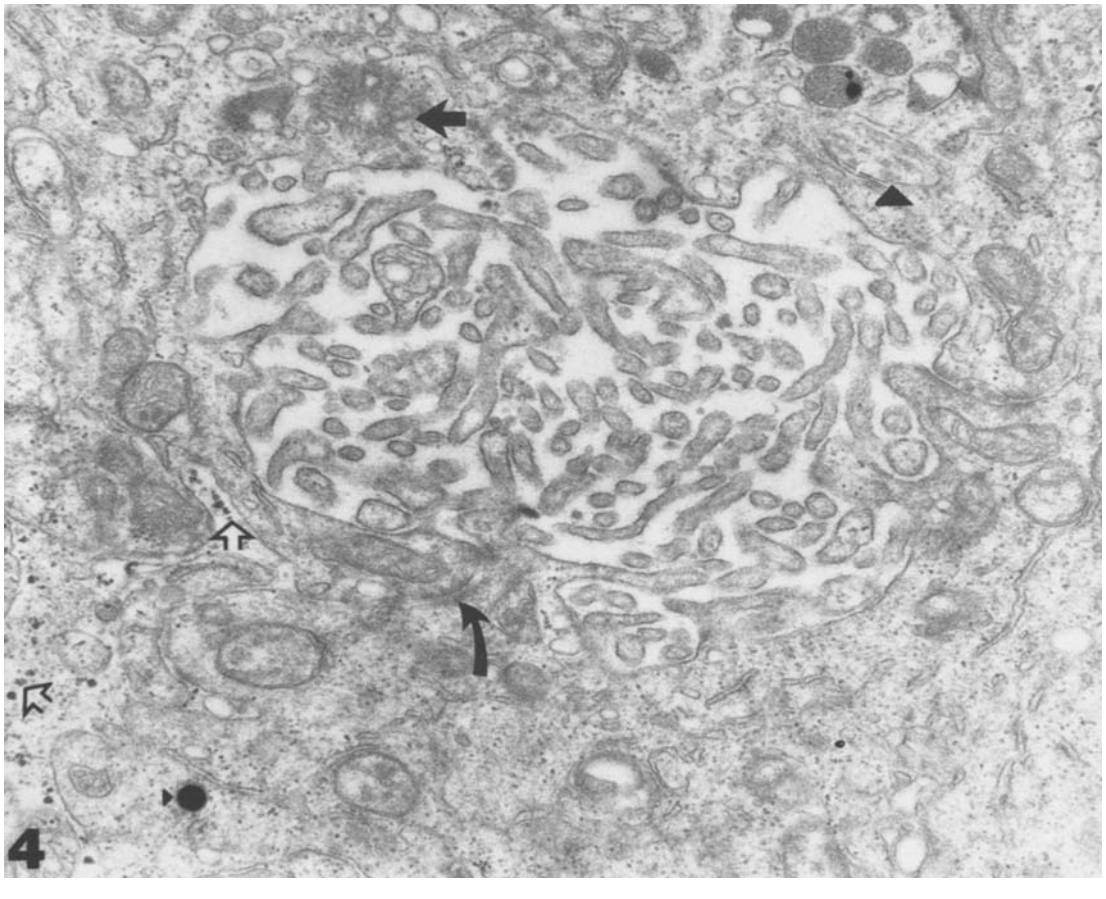

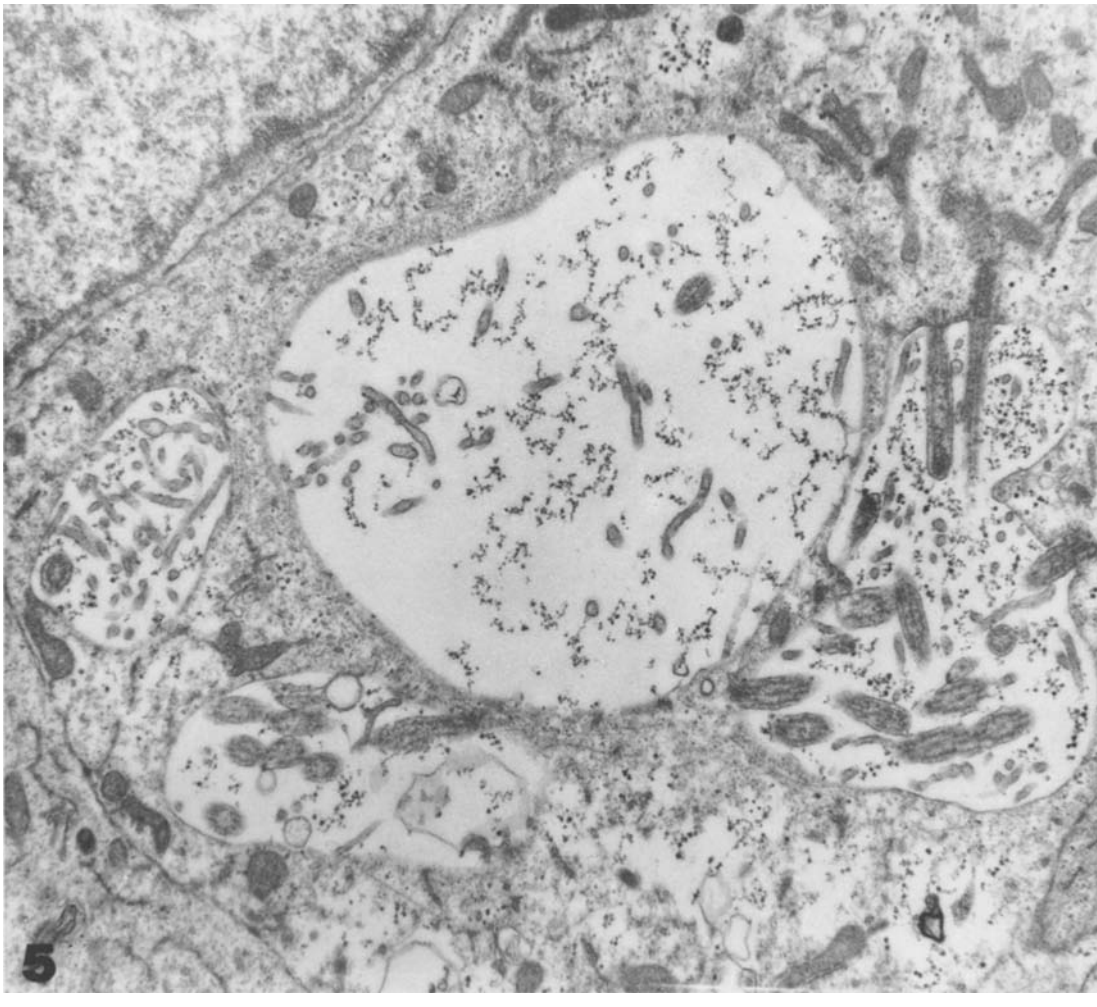

Figure 5. Multiple intracellular lumina filled with cilia, microvilli and glycogen. Slim cytoplasm bridges between adjacent compartments. Case 19, x 12.500.

filled parts of the perikaryon or even entire processes (Figures 7–9). Occasionally the concentrated glycogen was limited to the immediate vicinity of vessels.

Cilia were found in 9 cases; transversely sectioned they showed 9 peripheral and 2 central tubuli. Sometimes the cilia reach into the lumina of rosettes but more often they are found deep in the cytoplasm without contact with the plasma membrane (Figure 2). Malignant tumors often contain abortive cilia, which appear as a local perturbation of the plasma membrane without any differentiated internal tubular structure. Basal bodies and parts of the ciliary root system also occur in the absence of cilia.

◁ **Figure 4.** "True" rosette: lumen with microvilli, cilium (arrowhead), basal body (arrow), desmosome (curved arrow), dense body (small arrowhead) and glycogen (open arrows). Case 19, x 28.300.

Desmosomes occurred as isolated connections between cell processes, also connecting lateral surfaces of neighboring tumor cells with short wide segments. Differentiation between zonulae adhaerentes and zonulae occludentes was generally not possible in our material. In two spinal tumors (Figure 9), the plasma membrane of the tumor cell is also surrounded by a basal membrane. In cerebral ependyomas and tumors of the posterior cranial fossa, collagen could only be demonstrated in the perivascular space.

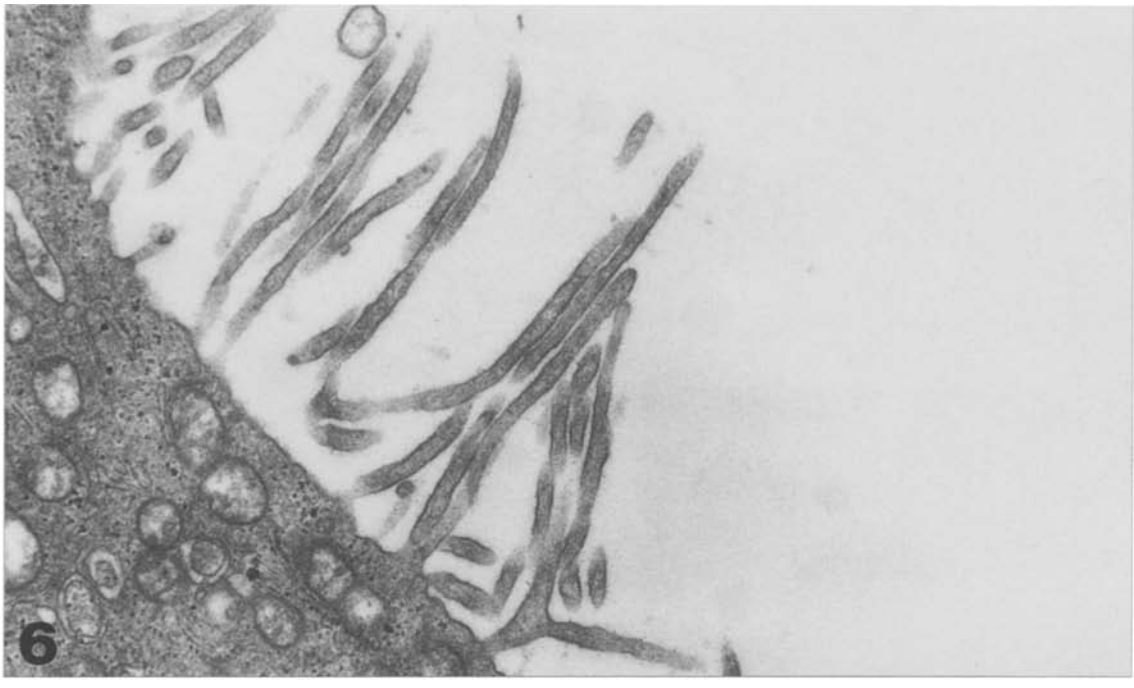
6

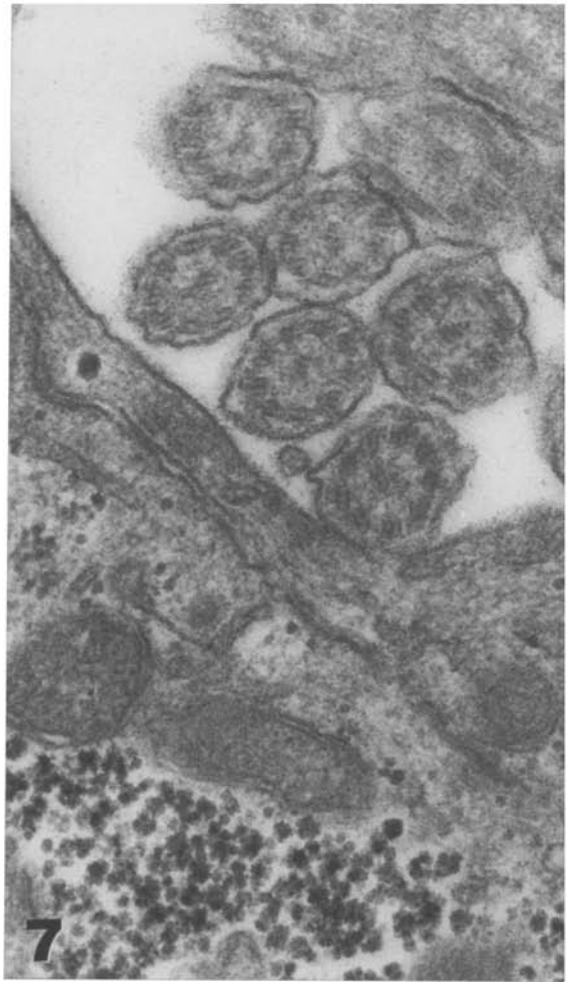
7

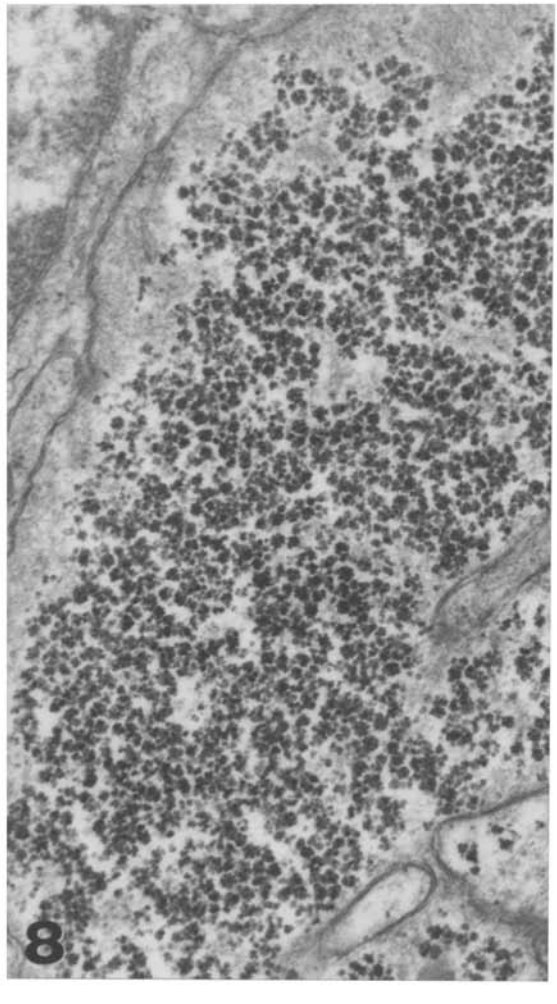
8

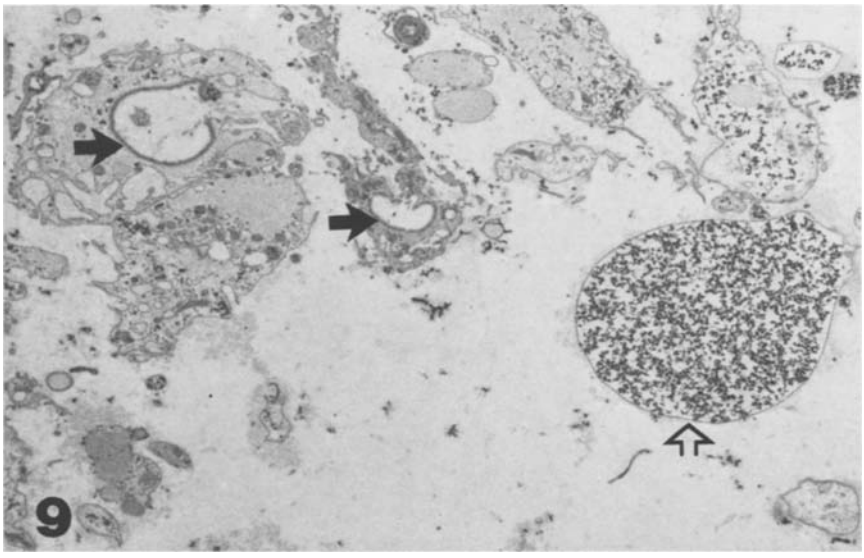

Figure 9. Cell invagination covered with basement membrane (arrow), glycogen (open arrow). Case 8, x 1.500.

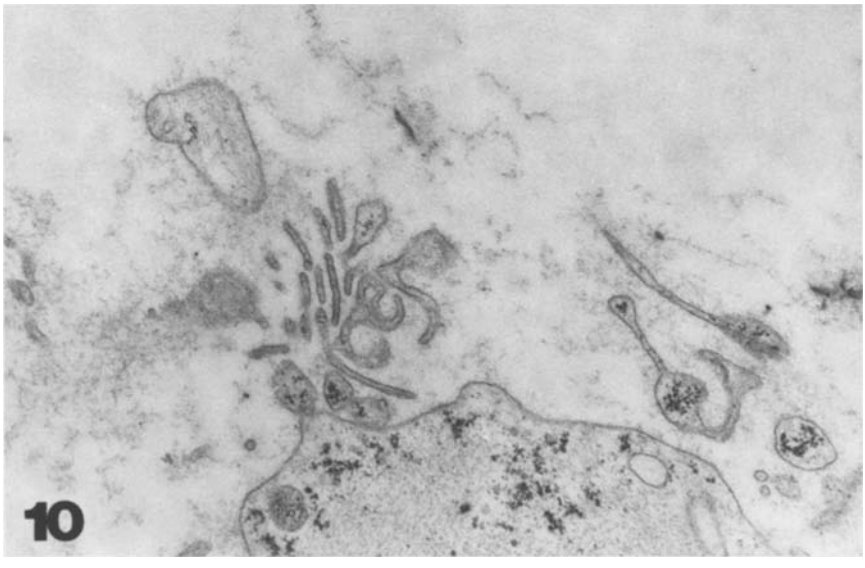

Figure 10. Microvilli and scattered glycogen granules. Case 8, x 8.000.

◁ **Figure 6.** Sparse glycogen underneath branching microvilli. Case 19, x 12.500.

Figure 7. Lumen formation with cilia, intracellular glycogen accumulation. Case 14, x 40.000.

Figure 8. Cell process filled with glycogen granules. Case 14, x 12.500.

4 Discussion

Ependymal brain tumors are generally defined according to conventional criteria on the basis of their localization in the vicinity of the ventricles, macroscopic findings and their typical histological picture of soma-free perivascular halos [33]. Problems in the diagnosis do, however, arise when there is an atypical localization, doubtfull macroscopic result or undifferentiated tissue.

In our material there were five tumors which fulfilled all criteria for real rosettes which are proof of the

diagnosis. RUBINSTEIN [28] already pointed out their relative rarity and emphasized that they are not an absolutely essential criterion. ZÜLCH [33] did not find any rosettes in cerebral tumors. In agreement with the literature, we must conclude that "true" rosettes are too seldom to be of much relevance in the electron microscopic diagnosis.

The electron microscope literature generally discribes modified ependymal cell patterns in rosette-like formations around very small lumina, which are not recognizable in the light microscope, especially in thick paraffin sections. Microvilli and disorganized cell contacts are usually present; they have been described as "rosette-like formations", "minirosettes" and "ultrastructural rosettes" [12, 13]. Quantitative data are lacking in the literature; only HIRANO and GHATAK [13] mention that rosettes are rare in malignant forms. We found ultrastructural rosettes in 9 cerebral and one spinal tumor. These ultrastructural rosettes are incomplete. Supratentorial tumors demonstrate a morphology which appears like an inadequate attempt to form a free surface, just failing to form an ependymal tube. Furthermore, ultrastructural rosettes are characteristic but not pathognomic for ependymomas. Intracytoplasmic lumen formation has also been observed in tuberous sclerosis [2] as well as in a subependymoma [23]. Both tumor types have been assumed to have partially ependymal origin [10].

Basement membranes which are formed by tumor cells independently of vessel mesenchyme have been demonstrated in myxopapillary cauda tumors [26] and ependymal cysts [14]. Our case 8 (Figure 9) demonstrates that a tumor variant with basement membranes can also occur at the thoracic level. In this particular case we are concerned with a relapsing tumor with regressive changes which could also be seen in the primary tumor.

Glycogen granules in their various morphological forms are the most common ultrastructural feature of our material. RUBIN et al. [27] pointed out the relatively high glycogen content in reactive ependymal cells, but did not find any glycogen in experimental ependymoblastomas. RAWLINSON et al. [26] described glycogen in spinal ependymomas. The electron microscope literaure does not mention the massive glycogen accumulation in cerebral ependymomas. This is even more noteworthy because glycogen analysis is one of the routine tests in neuropathological tumor diagnosis. The differential diagnosis should include the glycogen-positive Ewing sarcoma [17] and neuroblastoma [32]. Moss [24] found pools of glycogen granules in plexus papilloma, and according to that author glycogen may be lost during processing of the biopsy specimen. Some findings suggest that beta-granules may develop into branching filaments [29]. A close spatial relation of cilia and glycogen from a morphological point of view might suggest direct involvement of the carbohydrates into "manufacturing" of cilia and related structures. We are not aware of any biochemical analysis of human tissue regarding this problem. Recently massive glycogen accumulation has been described in the aging brain, and it was suggested that the aging process itself might lead to a disorder of carbohydrate metabolism [11].

After administration of psychotropic drugs like chlorpromazine there was pronounced accumulation of glycogen granules in pyramidal cells of rabbits [18, 19]. These drugs might inhibit the glycolytic metabolism in nerve cells. In our cases the medical treatment was unknown.

Microvilli, cilia and desmosomes are described as the major feature [6, 22]. GOEBEL and CRAVIOTO [12] observed that cilia usually project intracellularly, which is in agreement with our results. It may be worthwhile to study variants of abnormal cilia – this may have some impact on staging [15, 21].

Microvilli often appear to be pressed into the extracellular clefts or into the cytoplasm of tumor cells. Only serial sectioning can clarify the question of whether the latter localization is actually intracellu-

Table II. Summary of electron microscopic criteria. Order according to the frequency of positive features

	Case																			
	1	4	12	2	16	14	3	21	5	8	6	11	17	18	15	7	10	13	9	19	20
Desmosomes						+			+	+	+	+	+	+	+	+	+	+	+	+	+
Basal bodies					+			+			+	+	+	+	+			+	+	+	
Cilia			*	+								+	+	*	+	+		+	*	+	*
Microvilli							+	+	+	+		+	+			+	+			+	+
Glycogen					+	+	+	+	+	+	+			+	+	+	+	+	+	+	+
Typical Nuclei							+				+						+	+	+		+

*abortive cilia

lar or whether it is an invagination of the cell surface. The relatively frequent presence of microvilli in the tumor cells without any indication of a connection with the extracellular space suggests, however, an intracellular localization. A real ependymal tube with microvilli is much more seldom.

Generally we could not further classify desmosomes, probably due to the fact that the number of zonulae adhaerentes in malignant ependymomas is considerably reduced [31].

Friede and Pollack [9] and other authors describe a typical nuclear structure for ependymomas, but emphasize that this is not in itself a sufficient criterion for their identification. This is in agreement with our results. Nuclear inclusions are also nonspecific and have been seen in a number of gliomas [6, 20]. Their functional relevance is still unknown. Dense bodies are a common feature – it was speculated by Estes [8] that their appearance is associated with a better prognosis, but until now no data on this issue are avaible.

In Table II we have summarized the most important results for the confirmation of the diagnosis. When three or more positive criteria are present, then electron microscopy analysis may contribute significantly to the diagnosis. Fifteen tumors in our study fall into this category; 10 of these show ultrastructural rosettes and further characteristics of ependymal differentiation. Of particular interest is that 13 cases demonstrated glycogen, a marker which until now has not received adequate attention. Cases 1 and 4 do not show any ultrastructural features of ependymal differentiation. They thus do not permit an electron microscopic diagnosis, although histologically the diagnosis was unequivocal. Both cases were grade I tumors, and both patients were under 30 years of age. A further four tumors (cases 12, 2, 16, 14) each provided fewer than 3 positive ultrastructural features.

The negative electron microscopic results can be explained by methodological problems due to small samples for analysis as well as by histological factors. We are aware of another problem of our study: the amount of criteria in our samples depends on correct diagnosis, so our values might be underestimations.

Acknowledgment: We thank Verena Funke-Eckert for technical assistance and Dr. Margaret Davis for help in preparing the manuscript.

References

[1] Bailey P: A study of tumors arising from ependymal cells. Arch Neurol Psychiatr 11 (1924) 1–24
[2] Chadarevian J, R Hollenberg: Subependymal giant cell tumor of tuberose sclerosis. J Neuropathol Exp Neurol 38 (1979) 419–433
[3] Cruz-Sanchez F, J Cervós-Navarro, J Haustein, J Artigas: Ependymoblastomas: A pathological study. X Int Congr Neuropathol, Book of Abstracts No 308, Stockholm 1986
[4] Cruz-Sanchez F, J Haustein, ML Rossi, J Cervós-Navarro, J Hughes: Ependymoblastoma: A histological, immunohistological and ultrastructural study of 5 cases. Histopathology 12 (1988) 17-27.
[5] Cruz-Sanchez F, J Iglesias, ML Rossi, J Cervós-Navarro, J Figols, J Haustein: Histologic characterization of 41 ependymomas with the help of a personal computer. Cancer 62 (in press) 1988
[6] Dolmann C: Ultrastructure of brain tumors and biopsies. Praeger, New York 1984
[7] Erlandson R: Diagnostic transmission electron microscopy of human tumors. Masson, New York 1981
[8] Estes ML, LB Rorke: Cytoplasmic granules in ependymomas: a light and electron microscopic study. X Int Congr Neuropathol, Book of Abstracts No 309, Stockholm 1986
[9] Friede R, A Pollak: The cytogenetic basis for classifying ependymomas. J Neuropathol Exp Neurol 37 (1978) 103–118
[10] Fu Y, A Chen, S Kay, Y Young: Is subependymoma (subependymal glomerate astrocytoma) an astrocytoma or ependymoma? Cancer 34 (1974) 1992–2008
[11] Gertz HJ, J Cervós-Navarro, V Frydl, F Schultz: Glycogen accumulation of the aging human brain. Mech Ageing Dev 31 (1985) 25–35
[12] Goebel H, H Cravioto: Ultrastructure of human and experimental ependymomas. J Neuropathol Exp Neurol 34 (1972) 54–71
[13] Hirano A, N Ghatak: The fine structure of ependymoblastoma. J Neuropathol Exp Neurol 32 (1973) 144–152
[14] Hirano A, N Ghatak, H Wisoff, H Zimmermann: Comparative ultrastructural study of ependymoma and ependymal cyst. Am J Pathol 62 (1971) 11a
[15] Ho KL: Abnormal cilia in a fourth ventricular ependymoma. Acta Neuropathol 70 (1986) 30–37
[16] Horowitz ME, D Parham, E Douglass, L Kun, J Houghton, P Houghton: Development and characterization of human ependymoma xenograft HxBr5. Cancer Res 47 (1987) 499–504
[17] Katenkamp D, D Stiller, H Holzhausen: Morphologie des Neuroblastoms. Zentralbl Allg Pathol 127 (1983) 207–218
[18] Koizumi J, H Shiraishi: Ultrastructural appearance of glycogen in the hypothalamus of the rabbit following chlorpromazine administration. Exp Brain Res 10 (1970) 276–282
[19] Koizumi J, H Shiraishi: Ultrastructural appearance of glycogen in the hippocampus of the rabbit following

administration of psychotropic drugs. Exp Brain Res 13 (1971) 451–460
[20] Kroh H: Intranuclear inclusions in mouse neurons. Neuropatol Pol (in English) 22 (1984) 139–156
[21] Kubota T, J Ishise, T Yamashima, S Yamamoto: Abnormal cilia in a malignant ependymoma. Acta Neuropathol 71 (1986) 100–105
[22] Luse S: Electron microscopic studies of brain tumors. Neurology 10 (1960) 881–905
[23] Moss T: Observations on the nature of subependymoma: An electron microscopic study. Neuropathol Appl Neurobiol 10 (1984) 63–75
[24] Moss T: Tumours of the Nervous System. Springer, Berlin–Heidelberg–New York 1986
[25] Rahmann M, H Yeger, L Becker: A model of human primitive neuroectodermal tumor of the central nervous system. J Neurol Oncol 2 (1984) 270
[26] Rawlinson D, M Hermann, L Rubinstein: The fine structure of myxopapillary ependymoma of the filum terminale. Acta Neuropathol 25 (1973) 1–13
[27] Rubin R, C Sutton, H Zimmermann: Experimental ependymoblastoma. J Neuropathol Exp Neurol 27 (1968) 421–438
[28] Rubinstein L: Tumors of the central nervous system. AFIP, Bethesda 1972
[29] Suzuki Y, S Kamiya, K Ohta, S Suu: Lafora-like bodies in a cat: Case report suggestive of glycogen metabolism disturbances. Acta Neuropathol 48 (1979) 55–58
[30] Svien H, R Mabon, J Kernohan, K McWinchell: Ependymoma of the brain: Pathologic aspects. Neurology 3 (1953) 1–15
[31] Tani E, N Higashi: Intercellular junctions in human ependymomas. Acta Neuropathol 22 (1972) 295–304
[32] Yunis E, R Walpusk, J Agestini, J Hubbard: Glycogen in neuroblastomas. Am J Pathol 3 (1979) 313–323
[33] Zülch K: Biologie und Pathologie der Hirngeschwülste. Handbuch der Neurochirurgie Vol 3. Springer, Berlin 1956

Submitted December 10, 1987. Accepted January 4, 1988.

Dr. med. Jens Haustein
Institute for Neuropathology
Free University of Berlin
Hindenburgdamm 30
D-1000 Berlin 45, West Germany